Transverse mass distributions of protons produced in heavy-ion collisions at high energies*

XIE Wen-Jie(谢文杰)[1)]

Department of Physics, Yuncheng University, Yuncheng 044000, China

Abstract The transverse mass distributions of protons produced in Au-Au collisions at 8 A GeV and Pb-Pb collisions at 158 A GeV are calculated by using the Monte Carlo method in the framework of the multisource ideal gas model. It is found that our calculated results are in agreement with the experimental data in nucleus-nucleus collisions at high energies.

Key words transverse mass, multisource ideal gas model, Au-Au collisions, Pb-Pb collisions

PACS 25.75.Dw, 14.20.Jn

1 Introduction

The major character of high-energy heavy-ion collisions is to make nuclear matter to be at sufficiently high matter density and energy density in a short time [1–4]. We can use the heavy-ion beam which produces the nuclear matter at different densities to explore the equation of state and phase transition. Quantum chromodynamics (QCD) predicts that the excited nuclear matter at adequately high energy density and temperature will undergo a phase transition into a system of deconfined quarks and gluons (quark-gluon plasma, QGP) [5–11].

A great number of experimental data of heavy-ion collisions at high energies have been reported by now [12–22]. Meanwhile, many theoretical models are supposed to explain these data [23–30]. Explanation of transverse mass spectra of particles produced in collisions of heavy nuclei turns out to be one of the most difficult missions [31–33].

In this paper, we focus on the analysis of transverse mass spectra for protons produced in Au-Au collisions at 8 A GeV and Pb-Pb collisions at 158 A GeV based on the multisource ideal gas model [34–38]. To avoid the complex calculation in the analytic method, we will use the Monte Carlo method to calculate the transverse mass spectra and compare our calculated results with the experimental data of the E917 Collaboration [39–40] and the NA49 Collaboration [41].

2 The model

The multisource ideal gas model can be found in Refs. [34–38]. To give a whole presentation of this work, we introduce briefly the model as follows.

We establish a three-dimensional rectangular coordinate system and let the beam direction and the impact parameter be the Oz axis and Ox axis, respectively. Then, the xOz plane is the reaction plane. In high-energy heavy-ion collisions, a lot of emission sources of particles are assumed to form and many particles are emitted in each emission source. We suppose that the particles are isotropically emitted in the rest frame of the emission source.

According to the model [34–38], the three components p_x^*, p_y^* and p_z^* of particle momentum in the source rest system are assumed to obey a Gaussian distribution with the same standard deviation σ. Considering the expansion of emission source and interactions among emission sources, the particle momentum components p_x, p_y and p_z in the final state in the laboratory reference frame are respectively different from the particle momentum components p_x^*, p_y^* and p_z^* in the source rest frame. In line with the model [34–38], the relations between p_x and p_x^*, p_y

Received 11 January 2010

∗ Supported by National Natural Science Foundation of China (10975095, 10675077) and Natural Science Foundation of Shanxi Province (2007011005)

1) E-mail: wenjiexie@yeah.net

and p_y^*, as well as p_z and p_z^* are linear. We have

$$p_x = a_x p_x^* + b_x\sigma, \tag{1}$$

$$p_y = a_y p_y^* + b_y\sigma, \tag{2}$$

and

$$p_z = a_z p_z^* + b_z\sigma, \tag{3}$$

where a_x, b_x, a_y, b_y, a_z, and b_z are free coefficients, and σ is the parameter that denotes the width of the momentum distribution in the source rest system. In the final state, the transverse momentum and the transverse mass are defined by

$$p_{\rm T} = \sqrt{p_x^2 + p_y^2} \tag{4}$$

and

$$m_{\rm T} = \sqrt{p_{\rm T}^2 + m_0^2} \tag{5}$$

respectively, where m_0 is the rest mass of a particle.

In the Monte Carlo calculations, let R_1, R_2, R_3, and R_4 stand for even random variables distributed in [0, 1]. We have

$$p_x^* = \sqrt{-2\ln R_1}\cos(2\pi R_2)\sigma \tag{6}$$

and

$$p_y^* = \sqrt{-2\ln R_3}\cos(2\pi R_4)\sigma. \tag{7}$$

There is no longitudinal component of particle momentum because we do not need to take into account the longitudinal component in the investigation of transverse mass distribution. Considering Eqs. (1), (2), (4–7), the transverse mass can be written as

$$m_{\rm T} = \sigma\sqrt{\left[a_x\sqrt{-2\ln R_1}\cos(2\pi R_2) + b_x\right]^2 + \left[a_y\sqrt{-2\ln R_3}\cos(2\pi R_4) + b_y\right]^2 + m_0^2}\ . \tag{8}$$

In the above discussions, we can use Eq. (8) to calculate the transverse mass distributions by the Monte Carlo method, and five parameters can be obtained. The transverse mass distributions, $(1/2\pi m_{\rm T})\mathrm{d}^2N/\mathrm{d}m_{\rm T}\mathrm{d}y$ and $(1/m_{\rm T})\mathrm{d}^2N/\mathrm{d}m_{\rm T}\mathrm{d}y$, are finally obtained by the statistical method, where N and y denote the particle number and rapidity, respectively.

3 Comparison with experimental results

In Fig. 1, the transverse mass distributions, $(1/2\pi m_{\rm T})\mathrm{d}^2N/\mathrm{d}m_{\rm T}\mathrm{d}y$, of protons produced in Au-Au collisions at 8 A GeV, for the ten rapidity intervals and in the 0–5% central events, are indicated. The full circles denote the experimental data of the E917 Collaboration [39] and the curves represent our calculated results based on Eq. (8) by using the Monte Carlo method in the framework of a multisource ideal gas model [34–38]. From the top to bottom in Fig. 1, the spectra are multiplied by a factor of 10 for clarity. The parameter values of a_x, b_x, a_y, b_y and σ obtained by fitting the experimental data are shown in Table 1, and the method of χ^2-testing is used in the selection of parameter values. We see that our calculated results are in agreement with the experimental data of the E917 Collaboration [39].

The $(1/2\pi m_{\rm T})\mathrm{d}^2N/\mathrm{d}m_{\rm T}\mathrm{d}y$ distributions of protons produced in Au-Au collisions at 8 A GeV, for the ten rapidity intervals and in the 5%–12% central events, are denoted in Fig. 2. The full circles represent the experimental data of the E917 Collaboration [39] and the curves denote our calculated results from Eq. (8) by the Monte Carlo method. As for Fig. 1, the spectra are multiplied by a factor of 10 from the top to the bottom for clarity and the parameter values for the curves in Fig. 2 are shown in Table 1. In the selection of parameter values, the method of χ^2-testing is used. We see again that our calculated results are in agreement with the experimental data of the E917 Collaboration [39].

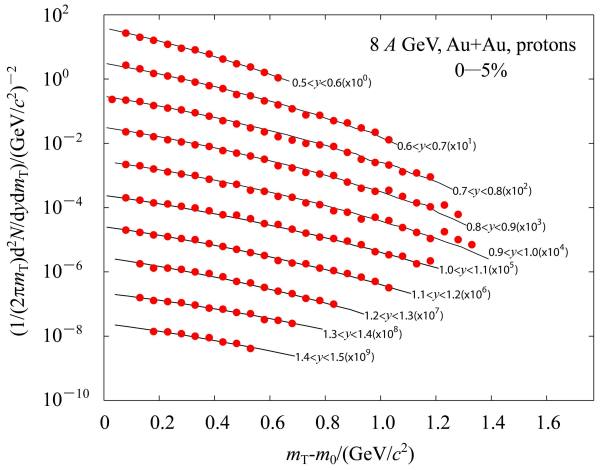

Fig. 1. The transverse mass distributions of protons produced in Au-Au collisions at 8 A GeV, for the ten rapidity intervals and in the 0–5% central events. The full circles denote the experimental data of the E917 Collaboration [39] and the curves represent our results.

In Figs. 3–5, the transverse mass distributions, $(1/2\pi m_{\rm T})\mathrm{d}^2N/\mathrm{d}m_{\rm T}\mathrm{d}y$, of protons produced in Au-Au collisions at 8 A GeV, for the ten rapidity intervals and the three classes of centrality, are given. The

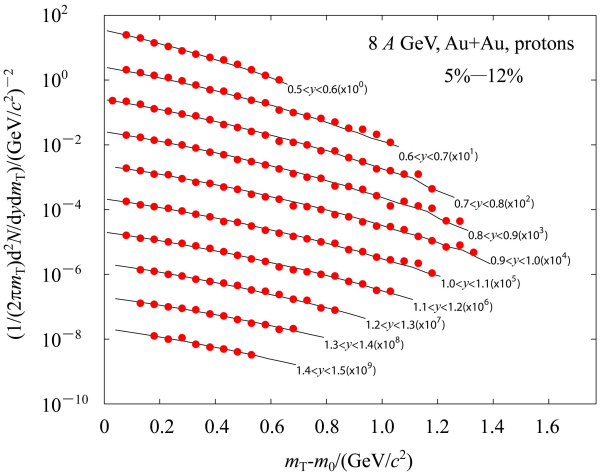

Fig. 2. As for Fig. 1, but displaying the results in the 5%–12% central events.

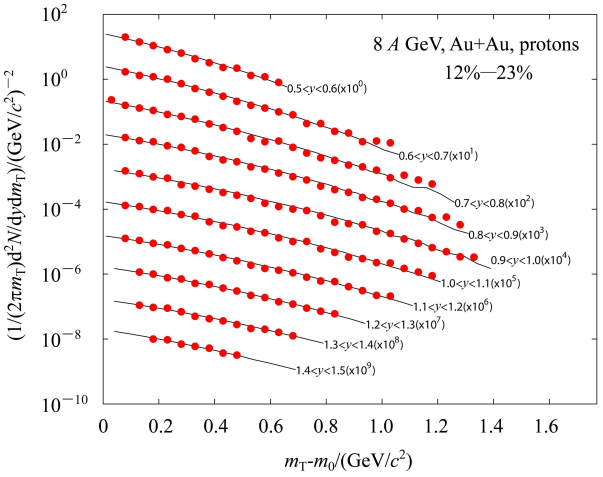

Fig. 3. As for Fig.1, but displaying the results in the 12%–23% central events.

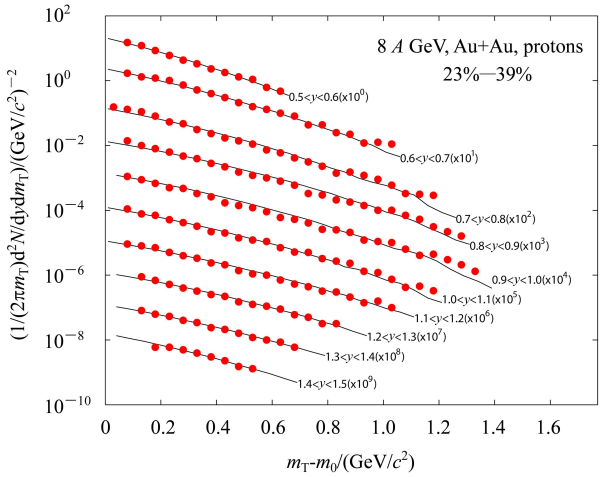

Fig. 4. As for Fig.1, but displaying the results in the 23%–39% central events.

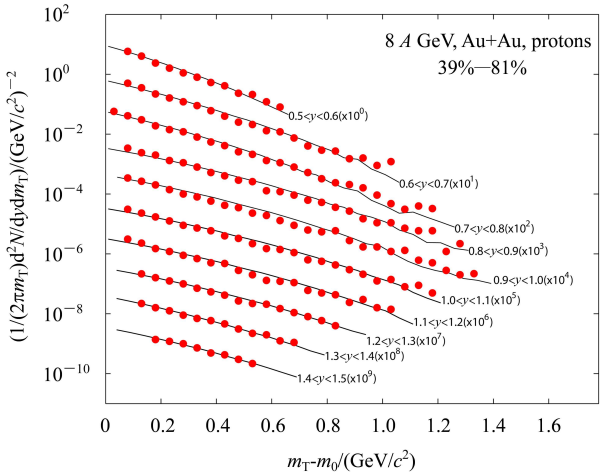

Fig. 5. As for Fig. 1, but displaying the results in the 39%–81% central events.

full circles denote the experimental data of the E917 Collaboration [39] and the curves represent our calculated results from the Monte Carlo method. From $0.5 < y < 0.6$ to $1.4 < y < 1.5$, the transverse mass spectra are scaled by successive powers of 10 as indicated, and the parameter values obtained by fitting the experimental data are shown in Table 1. Once more, the model results describe the experimental data.

The transverse mass distributions, $(1/m_{\rm T}){\rm d}^2N/{\rm d}m_{\rm T}{\rm d}y$, of protons produced in Pb-Pb collisions at 158 A GeV, for the six classes of centrality in the rapidity interval $2.4 < y < 2.8$, are indicated in Fig. 6. The full circles show the experimental data of the NA49 Collaboration [41] and the curves represent our calculated results from Eq. (8) by using the Monte Carlo

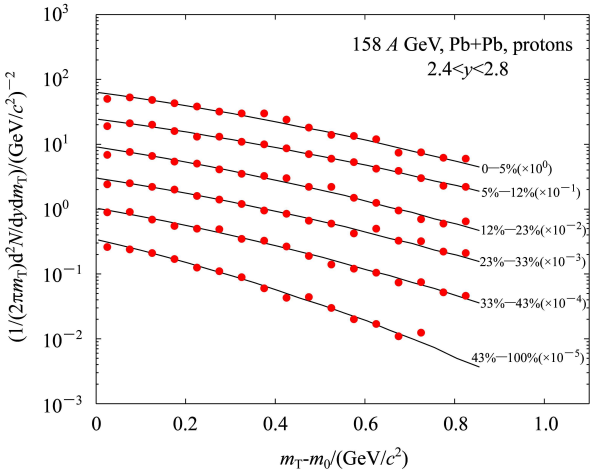

Fig. 6. The transverse mass spectra of protons produced in Pb-Pb collisions at 158 A GeV, for the six centrality classes and in the rapidity interval $2.4 < y < 2.8$. The full circles represent the experimental data of the NA49 Collaboration [41] and the curves show our results.

Table 1. Parameter values for curves in Figs. 1–5.

centrality	rapidity intervals	a_x	b_x	a_y	b_y	σ
0–5%	$0.5<y<0.6$	1.20	−0.05	1.25	−0.05	0.39
	$0.6<y<0.7$	1.25	−0.05	1.35	−0.05	0.41
	$0.7<y<0.8$	1.45	−0.05	1.35	−0.05	0.40
	$0.8<y<0.9$	1.35	−0.05	1.35	−0.05	0.42
	$0.9<y<1.0$	1.35	−0.05	1.42	−0.05	0.42
	$1.0<y<1.1$	1.50	−0.05	1.30	−0.05	0.43
	$1.1<y<1.2$	1.30	−0.05	1.45	−0.05	0.435
	$1.2<y<1.3$	1.30	−0.05	1.25	−0.05	0.45
	$1.3<y<1.4$	1.45	−0.05	1.40	−0.05	0.45
	$1.4<y<1.5$	1.50	−0.05	1.20	−0.05	0.46
5%–12%	$0.5<y<0.6$	1.20	−0.05	1.30	−0.05	0.38
	$0.6<y<0.7$	1.275	−0.05	1.25	−0.05	0.42
	$0.7<y<0.8$	1.40	−0.05	1.35	−0.05	0.40
	$0.8<y<0.9$	1.40	−0.05	1.35	−0.05	0.41
	$0.9<y<1.0$	1.43	−0.05	1.35	−0.05	0.42
	$1.0<y<1.1$	1.40	−0.05	1.35	−0.05	0.43
	$1.1<y<1.2$	1.40	−0.05	1.35	−0.05	0.435
	$1.2<y<1.3$	1.35	−0.05	1.25	−0.05	0.45
	$1.3<y<1.4$	1.30	−0.05	1.40	−0.05	0.45
	$1.4<y<1.5$	1.35	−0.05	1.20	−0.05	0.46
12%–23%	$0.5<y<0.6$	1.50	−0.05	1.40	−0.05	0.33
	$0.6<y<0.7$	1.20	−0.05	1.445	−0.05	0.38
	$0.7<y<0.8$	1.45	−0.1	1.23	−0.05	0.395
	$0.8<y<0.9$	1.44	−0.05	1.35	−0.05	0.40
	$0.9<y<1.0$	1.43	−0.05	1.30	−0.05	0.42
	$1.0<y<1.1$	1.42	−0.05	1.35	−0.05	0.42
	$1.1<y<1.2$	1.38	−0.05	1.35	−0.05	0.43
	$1.2<y<1.3$	1.35	−0.05	1.30	−0.05	0.435
	$1.3<y<1.4$	1.30	−0.05	1.35	−0.05	0.44
	$1.4<y<1.5$	1.35	−0.05	1.20	−0.05	0.44
23%–39%	$0.5<y<0.6$	1.35	−0.05	1.20	−0.05	0.36
	$0.6<y<0.7$	1.20	−0.05	1.45	−0.05	0.38
	$0.7<y<0.8$	1.24	−0.5	1.15	−0.05	0.40
	$0.8<y<0.9$	1.35	−0.05	1.40	−0.05	0.40
	$0.9<y<1.0$	1.30	−0.5	1.35	−0.5	0.38
	$1.0<y<1.1$	1.28	−0.05	1.30	−0.05	0.42
	$1.1<y<1.2$	1.37	−0.05	1.17	−0.05	0.44
	$1.2<y<1.3$	1.25	−0.05	1.30	−0.05	0.43
	$1.3<y<1.4$	1.35	−0.05	1.10	−0.05	0.44
	$1.4<y<1.5$	1.15	−0.05	1.10	−0.05	0.45
39%–81%	$0.5<y<0.6$	1.25	−0.05	1.20	−0.05	0.33
	$0.6<y<0.7$	1.25	−0.05	1.50	−0.05	0.33
	$0.7<y<0.8$	1.35	−0.05	1.20	−0.05	0.358
	$0.8<y<0.9$	1.38	−0.05	1.40	−0.05	0.37
	$0.9<y<1.0$	1.30	−0.05	1.30	−0.05	0.39
	$1.0<y<1.1$	1.40	−0.05	1.35	−0.05	0.38
	$1.1<y<1.2$	1.38	−0.05	1.33	−0.05	0.383
	$1.2<y<1.3$	1.25	−0.05	1.37	−0.05	0.387
	$1.3<y<1.4$	1.10	−0.05	1.35	−0.05	0.392
	$1.4<y<1.5$	1.30	−0.05	1.20	−0.05	0.387

method based on the multisource ideal gas model [34–38]. From 0–5% to 43%–100%, the transverse mass spectra are scaled by successive powers of 10, as indicated. The parameter values obtained by fitting the experimental data are shown in Table 2 and the χ^2-testing is used in the selection of parameter values. One can see that our calculated results by the Monte Carlo method are in agreement with the experimental data of protons produced in Pb-Pb collisions at high energy.

According to the multisource ideal gas model [34–38], a lot of emission sources are formed in heavy-ion collisions at high energies. We assume that there is a thermal equilibrium, or a local equilibrium among these emission sources in the final state. Then, we can give the $m_{\rm T}$ inverse slope parameter (T) by the following formula [42],

$$\sigma = \sqrt{\gamma m_0 T}, \tag{9}$$

where γ is the Lorentz factor.

In Fig. 7, the correlations between inverse slope parameter and rapidity for protons in Au-Au collisions at 8 A GeV are given. The full circles indicate the experimental data of the E917 Collaboration [40] and the hollow circles denote our calculated results. In the calculations, we have taken $\gamma \approx 1$. We can see that our calculated results by Eq. (9) are in agreement with the mean trend of the experimental data in Au-Au collisions at 8 A GeV. In the case of taking a great Lorentz factor, a lower $m_{\rm T}$ inverse slope will be obtained. It is difficult for us to give a precise Lorentz factor for the produced particles in the present work.

Table 2. Parameter values for curves in Fig. 6.

rapidity interval	centrality	a_x	b_x	a_y	b_y	σ
$2.4 < y < 2.8$	0–5%	1.30	−0.01	1.25	−0.01	0.53
	5%–12%	1.35	−0.01	1.25	−0.01	0.53
	12%–23%	1.25	−0.01	1.25	−0.01	0.51
	23%–33%	1.25	−0.01	1.25	−0.01	0.51
	33%–43%	1.25	−0.01	1.25	−0.01	0.48
	43%–100%	1.15	−0.01	1.15	−0.01	0.45

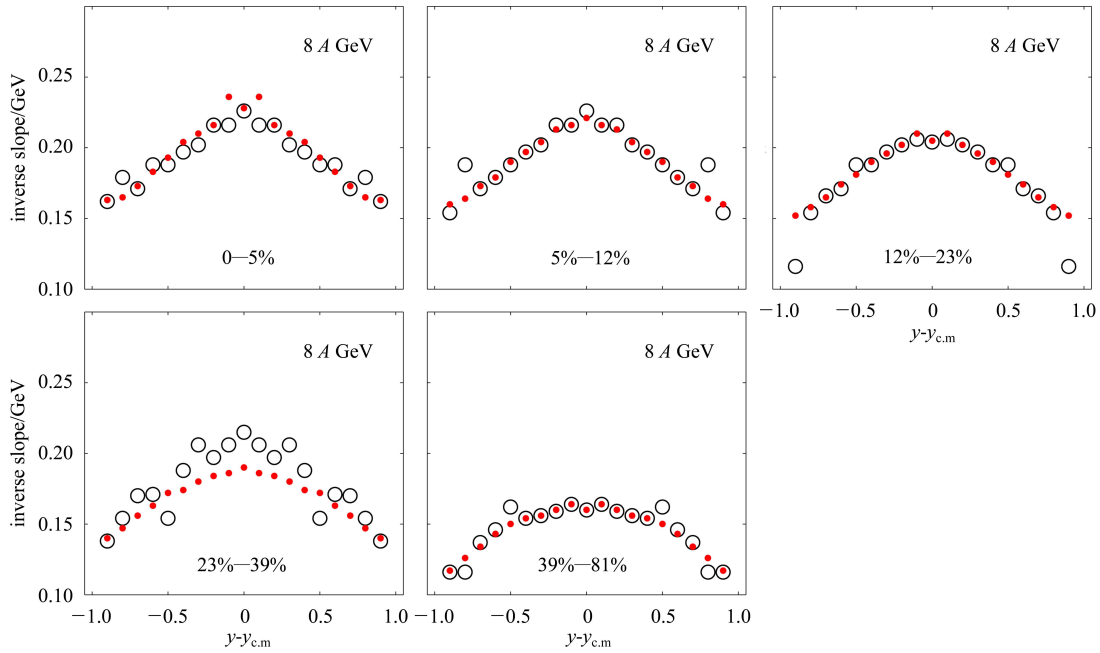

Fig. 7. The $m_{\rm T}$ inverse slope parameters of protons produced in Au-Au collisions at 8 A GeV as a function of rapidity. The percentage denotes the centrality. The full circles represent the experimental data of the E917 Collaboration [40] and the hollow circles display our calculated results.

Table 3. Inverse slope parameters of protons produced in Pb-Pb collisions at 158 A GeV, for the six classes of centralities in the rapidity interval $2.4 < y < 2.8$. The first line is our calculated results and the second line is the experimental data of NA49 Collaboration [41]. The statistical errors are shown in the experimental data.

0–5%	5%–12%	12%–23%	23%–33%	33%–43%	43%–100%
299	299	277	277	246	216
308±9	308±9	276±9	273±10	245±10	216±10

The $m_{\rm T}$ inverse slope parameters of protons produced in Pb-Pb collisions at 158 A GeV, for the six classes of centralities in the rapidity interval $2.4 < y < 2.8$, are shown in Table 3. The first line denotes the experimental data of the NA49 Collaboration [41] and the second line represents our results based on Eq. (9). In the calculations, we have taken $\gamma \approx 1$. One can see that our results are in line with the experimental data of protons produced in Pb-Pb collisions at 158 A GeV within the errors.

4 Conclusions and discussions

The transverse mass distributions, $(1/2\pi m_{\rm T}){\rm d}^2N/{\rm d}m_{\rm T}{\rm d}y$, of protons produced in Au-Au collisions at 8 A GeV, for the five classes of centralities and the ten rapidity intervals, and the transverse mass distributions, $(1/m_{\rm T}){\rm d}^2N/{\rm d}m_{\rm T}{\rm d}y$, of protons produced in Pb-Pb collisions at 158 A GeV, for the six classes of centralities in the rapidity interval $2.4 < y < 2.8$, have been studied by us in the framework of the multisource ideal gas model [34–38]. We have used the Monte Carlo method to calculate the transverse mass distributions and our calculations describe well the experimental data of the E917 Collaboration [39–40] and the NA49 Collaboration [41].

In Eq. (8), the parameters a_x and a_y denote an expansion of emission source along the Ox and Oy axes, and the parameters b_x and b_y can be used to describe a movement of the center of emission source in the Ox and Oy axes, respectively. From Table 1, we can see an expansion of the emission source along the positive x and positive y directions and a movement of the center of emission source along the negative x and negative y directions, respectively.

To understand the excitation degree of emission sources formed in heavy-ion collisions at high energies, we have calculated approximately the $m_{\rm T}$ inverse slope parameter of protons by Eq. (9) and found that our calculated results are in agreement with the mean trend of the experimental data of the E917 Collaboration [40] and the NA49 Collaboration [41].

The multisource ideal gas model is a reasonable picture in the description of high-energy heavy-ion collisions. A recent work [43] shows that the previous work of Liu et al. on the thermalized (two-)cylinder model [44–48] can be included in the framework of the multisource ideal gas model. However, the multisource ideal gas model has not considered the relativistic and/or quantum effects in many cases. For example, Eqs. (1)–(3) in Section 2 give only the mean relations between the two reference frames, but not a real reflection of the relativistic effect. We hope to improve the model in the frameworks of relativistic and quantum effects in our future work.

References

1 Ahle L, Akibak Y, Ashktorab K et al. Nucl. Phys. A, 1995, **590**: 249–258
2 Akiba Y, Ahle L, Ashktorab K et al. Nucl. Phys. A, 1996, **610**: 139–152
3 Ahle L, Akibak Y, Ashktorab K et al. Phys. Rev. C, 1998, **57**: R466–R470
4 Ludlam T, Mclerran L. Phys. Today., 2003, **56**: 48–54
5 Collins J C, Perry M J. Phys. Rev. Lett., 1975, **34**: 1353–1356
6 Baym G, Chin S A. Phys. Lett. B, 1976, **62**: 241–244
7 Freedman B, Mclerran L. Phys. Rev. D, 1978, **17**: 1109–1122
8 Shuryak E V. Phys. Rep., 1980, **61**: 71–158
9 Gross D J, Pisarski R D, Yaffe L G. Rev. Mod. Phys., 1981, **53**: 43–80
10 Staz H. Ann. Rev. Nucl. Part. Sci., 1985, **35**: 245–270
11 Mclerran L. Rev. Mod. Phys., 1986, **58**: 1021–1064
12 WANG S, Lisa M A, Albergo S et al. (EOS collaboration). Phys. Rev. Lett., 1996, **76**: 3911–3914
13 Partlan M D, Albergo S, Bieser F et al. (EOS collaboration). Phys. Rev. Lett., 1995, **75**: 2100–2103
14 HONG B, Kim Y J, Herrmann N et al. (FOPI collaboration). Phys. Rev. C, 2005, **71**: 034902
15 HONG B, Kim Y J, Herrmann N et al. (FOPI collaboration). Phys. Rev. C, 1998, **57**: 244–253
16 Förster A, Uhlig F, Böttcher I et al. (KAOS collaboration). Phys. Rev. Lett., 2003, **91**: 152301
17 Barrette J, Bellwied R, Bennett S et al. (E877 collaboration). Phys. Rev. C, 1997, **55**: 1420–1430
18 Barrette J, Bellwied R, Bennett S et al. (E877 collaboration). Phys. Rev. C, 2000, **63**: 014902
19 Klay J L, Ajitanand N N, Alexander J M et al. (E895 collaboration). Phys. Rev. C, 2003, **68**: 054905
20 Ahle L, Akibak Y, Ashktorab K et al. (E802 collaboration). Phys. Rev. C, 1999, **60**: 064901

21 Anticic T, Baatar B, Barna D et al. (NA49 collaboration). Phys. Rev. C, 2009, **79**: 044904
22 Aggarwal M M, Ahammed Z, Angelis A L S et al. (WA98 collaboration). Phys. Rev. Lett., 2004, **93**: 022301
23 Gustafson G. Nucl. Phys. A, 1994, **566**: 233–244
24 Werner K. Nucl. Phys. A, 1994, **566**: 477–481
25 Sorge H, Stöcker H, Greiner W. Nucl. Phys. A, 1989, **498**: 567–576
26 Sorge H, Von Keitz A, Mattiello R et al. Nucl. Phys. A, 1991, **525**: 95–103
27 Bravina L V, Amelin N S, Csernai L P et al. Nucl. Phys. A, 1994, **566**: 461–464
28 WANG X N. Phys. Rev. D, 1991, **43**: 104–112
29 PANG Y, Schlagel T J, Kahana S H. Phys. Rev. Lett., 1992, **68**: 2743–2746
30 Ornik U, Weinerand R M, Wilk G. Nucl. Phys. A, 1994, **566**: 469–472
31 Bratkovskaya E L, Soff S, Stöcker H. Phys. Rev. Lett., 2004, **92**: 032302
32 Wagner M, Larionov A B, Mosel U. Phys. Rev. C, 2005, **71**: 034910
33 Ga'zdzicki M, Gorenstein M I, Grassi F et al. Braz J Phys., 2004, **34**: 322–325
34 LIU Fu-Hu. Europhys Lett., 2003, **63**: 193–199
35 LIU Fu-Hu, Abd Allah N N, ZHANG Dong-Hai et al. Int. J Mod. Phys. E, 2003, **12**: 713–723
36 LIU Fu-Hu, Abd Allah N N, Singh B K. Phys. Rev. C, 2004, **69**: 057601
37 LIU Fu-Hu. Can. J Phys., 2004, **82**: 109–117
38 LIU Fu-Hu, LI Jun-Sheng, DUAN Mai-Ying. Phys. Rev. C, 2007, **75**: 054613
39 Back B B, Betts R R, CHANG J et al. (E917 collaboration). Phys. Rev. Lett., 2001, **86**: 1970–1973
40 Back B B, Betts R R, CHANG J et al. (E917 collaboration). Phys. Rev. C, 2002, **66**: 054901
41 Anticic T, Baatar B, Barna D et al. (NA49 collaboration). Phys. Rev. C, 2004, **69**: 024902
42 LIU Fu-Hu, SUN Han-Cheng. HEP & NP, 1994, **18**: 1073–1077 (in Chinese)
43 MENG Cai-Rong. Chin. Phys. Lett., 2009, **26**: 102501
44 LIU Fu-Hu, Panebratsev Y A. Nucl. Phys. A, 1998, **641**: 379–385
45 LIU Fu-Hu. Phys. Rev. C, 2002, **66**: 047902
46 LIU Fu-Hu. Phys. Lett. B, 2004, **583**: 68–72
47 LIU Fu-Hu, YUAN Ying, DUAN Mai-Ying. Nucl. Phys. A, 2008, **801**: 154–168
48 LIU Fu-Hu. Phys. Rev. C, 2008, **78**: 014902